AIP | Applied Physics Letters

Independent trapping and manipulation of microparticles using dexterous acoustic tweezers

Charles R. P. Courtney, Christine E. M. Demore, Hongxiao Wu, Alon Grinenko, Paul D. Wilcox, Sandy Cochran, and Bruce W. Drinkwater

Citation: Applied Physics Letters **104**, 154103 (2014); doi: 10.1063/1.4870489
View online: http://dx.doi.org/10.1063/1.4870489
View Table of Contents: http://scitation.aip.org/content/aip/journal/apl/104/15?ver=pdfcov
Published by the AIP Publishing

Independent trapping and manipulation of microparticles using dexterous acoustic tweezers

Charles R. P. Courtney,[1,a)] Christine E. M. Demore,[2] Hongxiao Wu,[2] Alon Grinenko,[3] Paul D. Wilcox,[3] Sandy Cochran,[2] and Bruce W. Drinkwater[3]
[1]*Department of Mechanical Engineering, University of Bath, Bath, United Kingdom*
[2]*Institute of Medical Science and Technology, University of Dundee, Dundee, United Kingdom*
[3]*Department of Mechanical Engineering, University of Bristol, Bristol, United Kingdom*

(Received 18 February 2014; accepted 12 March 2014; published online 17 April 2014)

An electronically controlled acoustic tweezer was used to demonstrate two acoustic manipulation phenomena: superposition of Bessel functions to allow independent manipulation of multiple particles and the use of higher-order Bessel functions to trap particles in larger regions than is possible with first-order traps. The acoustic tweezers consist of a circular 64-element ultrasonic array operating at 2.35 MHz which generates ultrasonic pressure fields in a millimeter-scale fluid-filled chamber. The manipulation capabilities were demonstrated experimentally with 45 and 90-μm-diameter polystyrene spheres. These capabilities bring the dexterity of acoustic tweezers substantially closer to that of optical tweezers. © *2014 AIP Publishing LLC*. [http://dx.doi.org/10.1063/1.4870489]

The ability to dexterously and independently manipulate multiple objects of microscale proportions is important to the biological sciences as this is the length scale of most biological cells. The use of the acoustic radiation force to trap cells at particular points is well established using devices operating at ultrasonic frequencies (see, for example, reviews by Laurell *et al.*[1] and Evander and Nilsson[2]). Dexterous acoustic manipulation of microparticles (acoustic tweezing) in 2D requires devices capable of trapping particles in an ultrasound field that can be modified or translated.

One approach to acoustic tweezing uses a highly focused single element ultrasonic transducer to produce a high frequency acoustic beam that acts to trap objects in a manner analogous to the focused laser beam in optical tweezers. This method has been used to trap 270-μm-diameter latex particles, frog eggs,[3] lipid droplets of 126-μm-diameter,[4] and leukemia cells.[5] An alternative acoustic method of generating a localized trap uses a resonant standing wave between an element of an ultrasonic linear array and a reflector and switching between elements. Linear arrays were first demonstrated to trap alumina particles in water[6] and have been applied in microfluidic systems with microparticles[7] and in air with large (centimeter scale) objects.[8] In a third approach, frequency variation allows the separation of nodes in a standing wave to be varied. Orthogonal standing surface acoustic waves have been used to trap microparticles (0.5 to 2 μm diameter) in a microfluidic channel. Varying the frequency of the applied signals (between 32.4 and 34 MHz) produced small changes in position.[9] A larger frequency range (18.5 to 37 MHz) allowed 10-μm-diameter polystyrene particles, bovine red blood cells, and *Caenorhabditis elegans* to be translated through an arbitrary path of several tens of micrometers.[10] Manipulation by varying the phase between opposing acoustic waves was first demonstrated in one dimension in a large tank.[11] Using ultrasonic transducers designed to minimize reflection allowed microparticles to be manipulated in one[12] and two[13] dimensions in millimeter scale chambers. Surface acoustic waves generated by opposing interdigital transducers have been used to achieve two-dimensional manipulation using phase control in a microchannel.[14] Both phase control and frequency variation of standing waves share the limitation that traps occur on a grid at half wavelength spacings and changes to phase or frequency affects all traps.

Most objects of interest in an acoustic trap are forced away from acoustic pressure maxima. In order to form traps, fields with a pressure minima surrounded by regions of high pressure amplitude must be generated. This property is characteristic of acoustic vortices. Acoustic vortices are functions that have a phase that rotates around their central axis, i.e., a dependence of $\exp(im\theta)$, where m is the topological charge and θ the azimuthal angle. Helicoidal beams (acoustic vortices that propagate along the central axis) have been used to transfer angular momentum to objects[15–17] and have been suggested as a method of trapping microparticles,[18] but trapping particles in such a manner has not been experimentally realized. There has been significant interest in the use of Bessel beams to apply negative radiation forces, i.e., axial forces in the direction opposing propagation.[19–21] Negative acoustic radiation forces have been demonstrated experimentally using centimeter scale targets and converging planar waves.[22] Recently, transverse forces have been calculated for Bessel beams of first order[23] and higher[24] with a view to developing improved acoustic tweezers operating in 3D.

Acoustic vortices (without propagation) can be used to provide lateral trapping and manipulation of microparticles constrained to a plane. It has been demonstrated that a Bessel function pressure field can be used to generate and manipulate a single acoustic trap.[25,26] Grinenko *et al.* showed theoretically that it is possible to generate and manipulate multiple traps of varying size.[27] The purpose of this work is to experimentally demonstrate trapping by superpositions of acoustic traps and by higher-order Bessel functions.

Figure 1(a) illustrates the device developed to manipulate microparticles. 64 piezoceramic elements operating at $f_0 = 2.35$ MHz, wavelength $\lambda = 640\,\mu$m in water, are arranged in a circle of diameter 10.98 mm. The region

a)c.r.p.courtney@bath.ac.uk

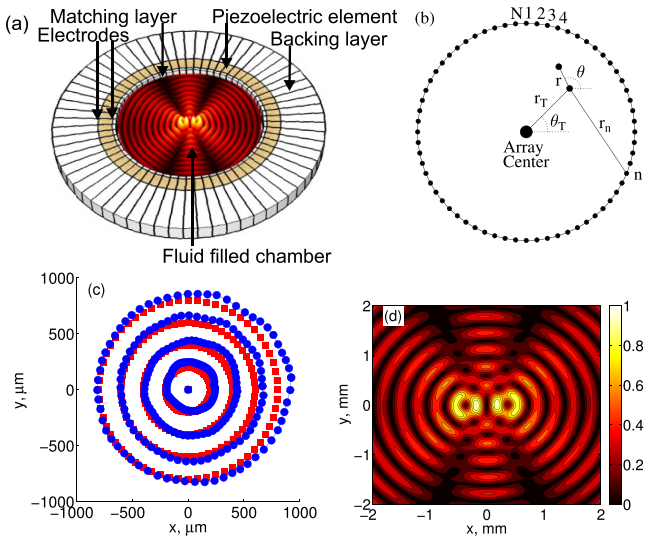

FIG. 1. (a) An isometric diagram of the 64 element circular array device used to manipulate particles. (b) A schematic showing the geometry and notation used in Eq. (1). Modeling and experimental results at 2.35 MHz ($\lambda = 640\ \mu$m). (c) The positions of a 90-μm-diameter particle as it is moved in concentric circles: actual positions (blue circles) and intended positions (red squares). (d) The pressure field in the chamber for a superposition of two $m = 1$ Bessel function traps, as calculated using a superposition of the outputs from all elements and ignoring reflections.

enclosed by the circle is sealed top and bottom with glass coverslips to produce a chamber, within which manipulation takes place. Each element has a matching layer on the inner (chamber-facing) surface and an absorbing backing layer on the outer surface. The use of these layers to minimize resonances in the chamber allows the pressure field within the chamber to be determined by setting appropriate values of amplitude and phase of sinusoidal signals applied to each element of the circular array of elements. A 1D transmission line model used to optimize the design indicates that the inclusion of the matching layer reduces the pressure-amplitude reflection coefficient for waves incident perpendicular to the front face to approximately 5%, from 70% without the layer. In order to prevent sedimentation, the chamber is half filled with agar, which acts as a substrate on which the microparticles are supported during manipulation. The remainder of the chamber is filled with water. For applications where use of agar would be problematic, acoustic levitation operating perpendicular to the plane of manipulation could be used.[26]

Bessel-function shaped fields were generated, in the array geometry illustrated in Figure 1(b), by applying to the sinusoidal array-element-driving signals the phase delays, ϕ_n, given by[26]

$$\phi_n = \left(\frac{2m\pi(n-1)}{N} - kr_n\right). \tag{1}$$

The $N = 64$ elements are labeled $n = 1,2,\ldots, N$, r_n is the distance from the desired trap center to element n, and m gives the order of the Bessel function approximated by the acoustic field. Bessel functions of order $m = 1$ and greater produce fields with pressure nodes at the target position, surrounded by cylindrically symmetrical pressure antinodes. These fields act to trap particles at the target position, which is determined by the second term in Eq. (1).

The area over which the acoustic pressure field can be controlled is determined by the number of elements, due to aliasing effects,[27] and the presence of unwanted resonances of the cavity which compete with the desired acoustic field. Courtney *et al.*[26] generated Bessel-function acoustic fields using a 16-element device which did not feature a matching layer and demonstrated that agglomerates of 10-μm-diameter polystyrene beads could be trapped and manipulated over a circular region with a radius of approximately one quarter wavelength. In this paper, the matching layer is designed to reduce unwanted resonances and 64 elements are used. This allows manipulation over a region whose radius exceeds the wavelength in the cavity. Figure 1(c) plots the location of a 90-μm-diameter polystyrene particle (Polysciences, Inc., Warrington, PA, USA) as it is manipulated in concentric rings. The trapped particle can be accurately manipulated throughout a circular region extending to 1 mm (1.6λ) from the center of the device. Beyond this region, the trap fails. The time taken for the sphere to respond to the change in acoustic field is of the order of tens of microseconds. A shift of $\lambda/4$ (160 μm) takes 80 ± 20 ms, an average velocity of 2.0 ± 0.3 mm/s, indicating a peak force of approximately 2 nN.

Generating multiple Bessel function shaped traps is achieved by calculating the applied signals for each desired trap according to Eq. (1) and then performing a linear superposition of the complex voltages required for each trap

$$V_n = V_0 \sum_{p=1}^{N_p} \exp\left(\frac{2im\pi(n-1)}{N} - ikr_{pn}\right), \tag{2}$$

where there are N_p traps and r_{pn} is the distance from the nth element to the pth trap. V_0 is the voltage amplitude for each element of a single trap. The maximum voltage amplitude $|V_n|$ is experimentally limited to 25 V, and the amplitude of each trap, V_0, must be scaled appropriately. Figure 1(d) shows the calculated pressure field for two traps separated by 800 μm, calculated from the superposition of the fields from each element, with amplitudes and phases determined by the applied electrical signal. The solution for each element is calculated using the far field approximation and reflections are neglected. If the separation between traps is too small, the interference restricts manipulation. For $m = 1$ traps, the first maximum of the Bessel function occurs at 0.3λ, so that bringing the traps to a separation of 0.6λ (380 μm at $f_0 = 2.35$ MHz) can lead to complete cancellation of the fields and loss of trapping.

In Figure 2, two particles are moved simultaneously along parallel paths separated by 800 μm in opposite directions (the particle on the left in the negative y direction and the particle on the right in the positive y direction). The actual path followed deviates from the ideal path by up to 130 μm. The model, which excludes reflections, predicts the qualitative behavior of the device well, indicating that the variations in the path shown are a result of the interference between the two traps. See supplementary material for the model generated pressure fields used to predict the particle paths.[28]

Traps with the first pressure maxima at larger distances from their centers can be generated using higher-order Bessel functions. Figures 3(a)–3(c) show modeled pressure fields for

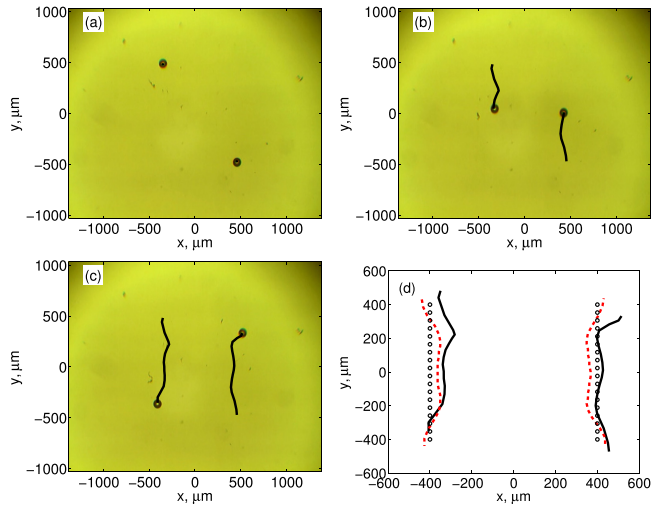

FIG. 2. Two 90-μm-diameter particles on an agar substrate in the manipulation chamber. The microparticles are simultaneously moved through 800 μm. (a) Particles trapped at a separation of 1130 μm. (b) and (c) Particles moved along parallel paths, separated by 800 μm. In (b), each particle has been moved 400 μm and in (c) each has been moved 800 μm. The path followed by each particle is overlaid in black. (d) The paths of the particles (black lines) are shown with the desired paths (black circles) and the paths of each particle predicted by the model of the acoustic field produced by the array (red dashed lines). (Multimedia view) [URL: http://dx.doi.org/10.1063/1.4870489.1]

Bessel functions of order 7, 3, and 1, respectively, generated by changing the value of m in Eq. (1). As order increases, the size of the central trap grows, with a flat central region of low pressure amplitude surrounded by a region of higher pressure amplitude. Figures 3(d)–3(f) show the effect of these fields on 45-μm-diameter beads on an agar layer. Figure 3(d) shows the response of the particles to $m = 7$ Bessel function. Particles that were located closer than 870 μm ($= 1.36\lambda$ at $f_0 = 2.35$ MHz) to the center before the field was switched on were trapped within the central trap of the field. Reducing the order of the Bessel function reduces the radius of the first maximum, and the size of the central trap, and particles can be progressively forced to the center. The still images shown in Figure 3 are taken from a series of steps where particles were swept into a single trap by reducing the Bessel function order from $m = 7$ to $m = 6$ and so on, down to $m = 1$.

Particles in separate first-order-Bessel-function traps cannot be brought together by simply moving the traps together as interference causes traps in close proximity to fail. However, particles can be manipulated in individual traps and then trapped in a single higher order trap and brought together by reducing the trap size. Figure 4 shows this process applied to three microparticles. In Figure 4(a), particles have been trapped in three $m = 1$ traps each is 400 μm from the device center. Figures 4(b) and 4(c) show the trap locations being rotated through $2\pi/3$, so that each trap moves to the

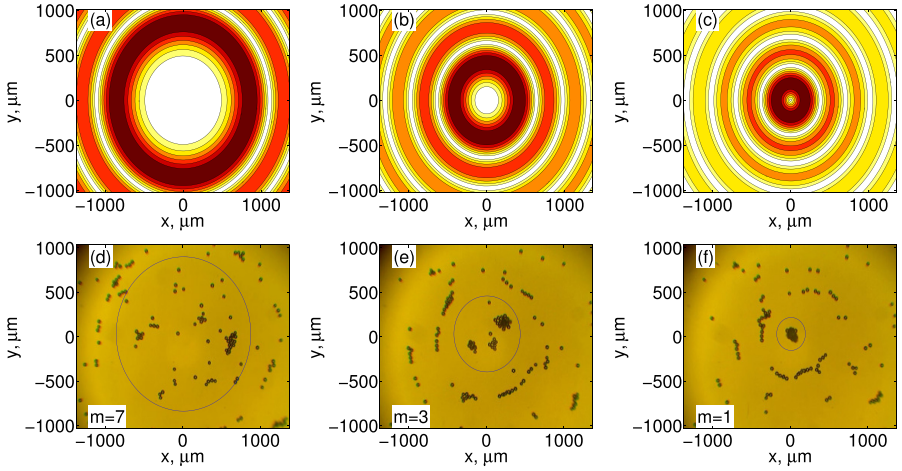

FIG. 3. Trapping of 45-μm-diameter polystyrene beads using higher order Bessel functions. (a)–(c) show the modeled pressure fields for the $m = 7$, 3, and 1 cases, respectively, and (d)–(f) show the resulting distribution of particles. In each case, the overlaid circle shows the location at which the pressure maximum for that order of Bessel function would be expected. (Multimedia view) [URL: http://dx.doi.org/10.1063/1.4870489.2]

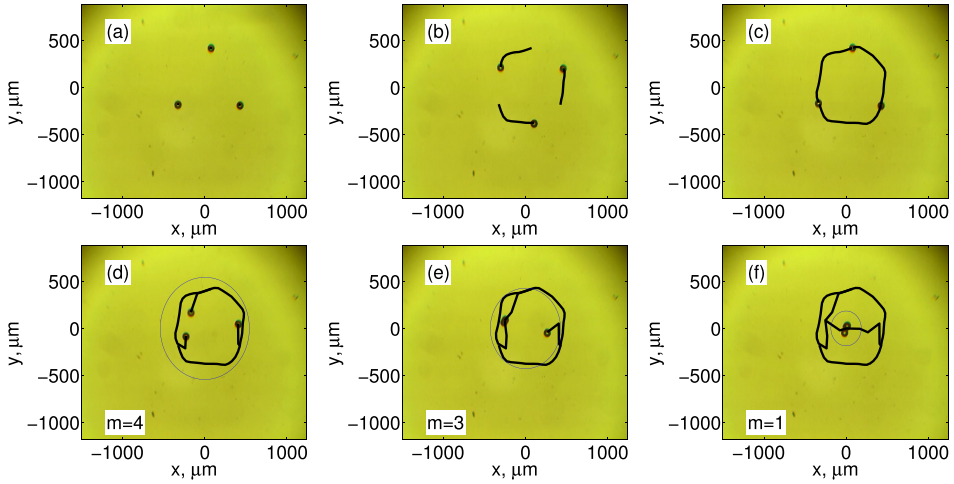

FIG. 4. Three particles being manipulated and then brought together. (a) Three particles each trapped 400 μm from the center of the device. (b) Each particle having being moved through $\pi/3$ radians with lines showing path followed. (c) Each particle having being moved through $2\pi/3$ radians. All three particles were then trapped in a single $m = 5$ trap and then the order is reduced one step at a time to $m = 1$. (d)–(f) show the $m = 4$, $m = 3$, and $m = 1$ stages, respectively, with the particle paths and first maxima plotted. (Multimedia view) [URL: http://dx.doi.org/10.1063/1.4870489.3]

location originally occupied by its neighbor. The three traps are then replaced with a single $m = 5$ Bessel function at the center of the chamber. The first maximum of this trap occurs at 540 μm (0.85λ) radius from the trap center. To bring the particles together, the order is reduced. Figures 4(d)–4(f) show the $m = 4$, $m = 3$, and final $m = 1$ cases, respectively. All three particles are eventually trapped at the center of the device in Figure 4(f).

Acoustic tweezers using circular arrays to generate acoustic traps, controlled electronically by varying the phase and amplitude of the electrical signal applied to each element, offer a relatively simple method of manipulating microscale objects dexterously. Using a 64-element circular array with matching layers designed to reduce unwanted resonances this work has demonstrated that manipulation is possible over a significant region and two other capabilities are available: microparticles spread over a plane can be brought together into a single trap by progressively generating traps of decreasing size and particles separated by more than 0.6λ (0.38 mm) can be trapped in separate traps and manipulated independently within a region extending 1.6λ (1 mm) from the center of the array.

These capabilities bring the dexterity of acoustic tweezers substantially closer to that of optical tweezers. Acoustic tweezers have the additional benefits of being capable of operating on larger objects and on a wider range of materials, with less expensive and less complicated equipment and using lower power densities.

This work has been funded by the Engineering and Physical Science Research Council, UK through the Electronic Sonotweezers programme (Grant No. EP/G012067/1). The authors thank G. Dasey, D. Martin, and J. Gove at the University of Dundee for their assistance in fabricating the array.

[1]T. Laurell, F. Petersson, and A. Nilsson, Chem. Soc. Rev. **36**, 492 (2007).
[2]M. Evander and J. Nilsson, Lab Chip **12**, 4667 (2012).
[3]J. R. Wu, J. Acoust. Soc. Am. **89**, 2140 (1991).
[4]J. Lee, S. Y. Teh, A. Lee, H. H. Kim, C. Lee, and K. K. Shung, Appl. Phys. Lett. **95**, 073701 (2009).
[5]J. Lee, C. Lee, H. H. Kim, A. Jakob, R. Lemor, S.-Y. Teh, A. Lee, and K. K. Shung, Biotechnol. Bioeng. **108**, 1643 (2011).
[6]T. Kozuka, T. Tuziuti, H. Mitome, and T. Fukuda, Jpn. J. Appl. Phys., Part 1 **37**, 2974 (1998).
[7]P. Glynne-Jones, C. E. M. Demore, C. W. Ye, Y. Q. Qiu, S. Cochran, and M. Hill, IEEE Trans. Ultrason. Ferroelectr. Freq. Control **59**, 1258 (2012).
[8]D. Foresti, M. Nabavi, M. Klingauf, A. Ferrari, and D. Poulikakos, Proc. Natl. Acad. Sci. U. S. A. **110**, 12549 (2013).
[9]C. D. Wood, J. E. Cunningham, R. O'Rorke, C. Walti, E. H. Linfield, A. G. Davies, and S. D. Evans, Appl. Phys. Lett. **94**, 054101 (2009).
[10]X. Ding, S.-C. S. Lin, B. Kiraly, H. Yue, S. Li, I. K. Chiang, J. Shi, S. J. Benkovic, and T. J. Huang, Proc. Natl. Acad. Sci. U. S. A. **109**, 11105 (2012).
[11]T. Kozuka, T. Tuziuti, H. Mitome, T. Fukuda, and F. Arai, "Control of position of a particle using a standing wave field generated by crossing sound beams," in *Proceedings of the 1998 IEEE Ultrasonics Symposium* (IEEE, New York, 1998), Vols. 1 and 2, pp. 657–660.
[12]C. R. P. Courtney, C. K. Ong, B. W. Drinkwater, P. D. Wilcox, C. Demore, S. Cochran, P. Glynne-Jones, and M. Hill, J. Acoust. Soc. Am. **128**, E195 (2010).
[13]C. R. P. Courtney, C. K. Ong, B. W. Drinkwater, A. L. Bernassau, P. D. Wilcox, and D. R. S. Cumming, Proc. R. Soc. A **468**, 337 (2012).
[14]L. Meng, F. Cai, J. Chen, L. Niu, Y. Li, J. Wu, and H. Zheng, Appl. Phys. Lett. **100**, 173701 (2012).
[15]K. D. Skeldon, C. Wilson, M. Edgar, and M. J. Padgett, New J. Phys. **10**, 013018 (2008).
[16]K. Volke-Sepulveda, A. O. Santillan, and R. R. Boullosa, Phys. Rev. Lett. **100**, 024302 (2008).
[17]C. E. M. Demore, Z. Yang, A. Volovick, S. Cochran, M. P. MacDonald, and G. C. Spalding, Phys. Rev. Lett. **108**, 194301 (2012).
[18]S. T. Kang and C. K. Yeh, IEEE Trans. Ultrason. Ferroelectr. Freq. Control **57**, 1451 (2010).
[19]P. L. Marston, J. Acoust. Soc. Am. **120**, 3518 (2006).
[20]F. G. Mitri, J. Phys. A: Math. Theor. **42**, 245202 (2009).
[21]P. L. Marston, J. Acoust. Soc. Am. **125**, 3539 (2009).
[22]C. E. M. Demore, P. M. Dahl, Z. Yang, P. Glynne-Jones, A. Melzer, S. Cochran, M. P. MacDonald, and G. C. Spalding, "An acoustic tractor beam," Phys. Rev. Lett. (to be published).
[23]G. T. Silva, J. H. Lopes, and F. G. Mitri, IEEE Trans. Ultrason. Ferroelectr. Freq. Control **60**, 1207 (2013).
[24]D. Baresch, J. L. Thomas, and R. Marchiano, J. Appl. Phys. **113**, 184901 (2013).
[25]A. L. Bernassau, C. R. P. Courtney, J. Beeley, B. W. Drinkwater, and D. R. S. Cumming, Appl. Phys. Lett. **102**, 164101 (2013).
[26]C. R. P. Courtney, B. W. Drinkwater, C. E. M. Demore, S. Cochran, A. Grinenko, and P. D. Wilcox, Appl. Phys. Lett. **102**, 123508 (2013).
[27]A. Grinenko, P. D. Wilcox, C. R. P. Courtney, and B. W. Drinkwater, Proc. R. Soc. A **468**, 3571 (2012).
[28]See supplementary material at http://dx.doi.org/10.1063/1.4870489 for the model generated pressure fields used to predict the particle paths.